

LA-UR - 74-1716

654-741136--1

TITLE: NEUTRON DIFFRACTION STUDIES OF DEUTERIUM
SOLID STRUCTURES AND TRANSITIONS

AUTHOR(S): J. L. Yarnell, R. L. Mills, A. F. Schuch

SUBMITTED TO: International Conference on Quantum Crystals
Tbilissi, USSR, 11-15 November 1974


By acceptance of this article for publication, the publisher recognizes the Government's (license) rights in any copyright and the Government and its authorized representatives have unrestricted right to reproduce in whole or in part said article under any copyright secured by the publisher.

The Los Alamos Scientific Laboratory requests that the publisher identify this article as work performed under the auspices of the U. S. Atomic Energy Commission.

MASTER

NOTICE

This report was prepared as an account of work sponsored by the United States Government. Neither the United States nor the United States Atomic Energy Commission, nor any of their employees, nor any of their contractors, subcontractors, or their employees, makes any warranty, express or implied, or assumes any legal liability or responsibility for the accuracy, completeness or usefulness of any information, apparatus, product or process disclosed, or represents that its use would not infringe privately owned rights.


los alamos
scientific laboratory
of the University of California
LOS ALAMOS, NEW MEXICO 87544

Neutron Diffraction Studies of Deuterium

Solid Structures and Transitions*

J. L. Yarnell, R. L. Mills, and A. F. Schuch
University of California, Los Alamos Scientific Laboratory
Los Alamos, New Mexico 87544, U.S.A.

ABSTRACT

Fine-grained, randomly-oriented samples of solid D_2 were prepared by injecting D_2 gas into liquid He at 4 K. Para ($J = 1$) concentrations of 2%, 29%, and 96% were used. In all cases, the as-frozen solid was predominantly fcc, with $\sim 10\%$ of the material in the hcp form expected at 4 K. Upon annealing at ~ 12 K, all samples transformed to pure hcp, and remained hcp when returned to 4 K. As expected, only the 96% para samples transformed to a cubic phase upon cooling to 1.5 K. However, the transition did not go to completion and neither holding for many hours at 1.5 K nor cycling between 1.5 K and 4 K would make it do so. This behavior confirms earlier observations that the transition is martensitic. Careful analysis of the data, using cross-correlation techniques, revealed the presence of very weak, mixed-index peaks characteristic of the ordered Pa3 structure. Evidence of stacking faults (peak broadening and, for fcc, peak shifts) was seen for all structures. The average number of planes between faults was ~ 14 for the as-frozen fcc, ~ 95 for the annealed hcp, and ~ 27 for the Pa3. At 4 K, the molar volumes of the as-frozen fcc and the annealed hcp were the same within the experimental accuracy, and there was no observable volume change when the 2% and 29% para hcp samples were cooled from 4 K to 1.5 K. These molar volumes are given by $V = 19.998 - 0.203x \pm 0.013 \text{ cm}^3/\text{mol}$, where x is the para-concentration. The molar volume for the Pa3 at 1.5 K was $19.681 \pm 0.007 \text{ cm}^3/\text{mol}$, with $x = 0.96$. For the annealed hcp, the c/a ratio was smaller than ideal by 1 part in 1200. For all structures, the observed intensities of the diffraction peaks were in good agreement with calculations based on wave functions for free D_2 molecules in $J = 0$ and $J = 1$ rotational states.

*Work performed under the auspices of the U.S. Atomic Energy Commission.

These experiments were carried out on solid deuterium, since it is the most favorable of the hydrogen isotopes for neutron diffraction studies. The work will be described in terms of this isotope, although most of the discussion also applies to the lighter isotope. Some of the results were reported at the LT 13 Conference on Low Temperature Physics.⁽¹⁾

Deuterium molecules may be described as rigid rotators, even in the solid, since the anisotropic interactions are small compared to the spacing of the rotational energy levels. At low temperatures, the molecules will be in the lowest accessible rotational state: $J = 0$ for ortho-deuterium or $J = 1$ for para-deuterium. The $J = 0$ state is non-degenerate and spherically symmetric. It is therefore incapable of any orientational ordering. However, the $J = 1$ state is threefold degenerate, with $m_J = \pm 1$ or 0. Since anisotropic interactions between $J = 1$ molecules may lift this degeneracy, orientational ordering into one of the substates may take place for high $J = 1$ concentrations and low temperatures. In the absence of long-range order, $J = 1$ molecules are indistinguishable from spheres as far as the coherent scattering of radiation is concerned.

A simplified phase diagram for deuterium, based on the results of many measurements, is shown in Fig. 1. The solid freezes from the liquid with the molecular centers of mass in a hexagonal-closed-packed (hcp) lattice. There is no evidence of long-range ordering in this structure. At low temperatures and high para-concentrations, there is a phase change to a structure with centers of mass on a face-centered cubic (fcc) lattice. The $J = 1$ molecules are ordered: the most likely space group is believed to be $Pa\bar{3}$ (T_h^6), in which the molecules are in the $J = 1$, $m_J = 0$ state with

respect to quantization axes along the cube diagonals. There are four sublattices, one for each of the four body diagonals of the cube.

When we undertook our measurements, the existing direct diffraction evidence that the ordered cubic state was indeed Pa3 was somewhat inconclusive. Mucker, Harris, White, and Erickson⁽²⁾ had obtained neutron diffraction data on 80% para-deuterium at 1.9 K. To avoid large preferentially oriented grains, the samples were frozen in the pores of an aluminum sponge. Unfortunately the sponge gave rise to diffraction lines that tended to mask those from the sample. Two weak peaks were identified as the (210) and (211) reflections of the Pa3 space group, and were cited as evidence for this structure. The intensities of these peaks depend critically on the subtraction of background peaks that appear at similar angles. The reported intensities are in good agreement with those calculated for classical molecules fixed along the four cube diagonals. However, this model is much too localized and when a quantum mechanical calculation is made⁽¹⁾, the probability density distribution for the $J = 1, m_J = 0$ state reduces the expected intensities by nearly an order of magnitude. This observation has also been made by Werner Press.⁽³⁾

We developed an improved technique for producing randomly-oriented, fine-grained samples free of background structure. Deuterium gas with 2, 29, and 96% para-concentration was injected into boiling helium contained in a cell made from a titanium-zirconium alloy chosen to have zero coherent scattering cross-section for neutrons. Liquid helium

remained in the interstices of the sample and provided thermostatic cooling in the range 1.5 to 4 K without contributing significantly to the diffraction pattern. When the liquid was boiled away the sample temperature rose to around 12 K.

Our procedure of quenching deuterium gas in liquid helium raises the question of whether helium atoms might condense in the deuterium lattice at a sufficient number of impurity sites to modify the solid structures and transitions.

We are unaware of any direct studies of the solid solubility of He in the hydrogens but extensive measurements have been made of the solubility of He gas in liquid $n\text{-H}_2$ ⁽⁴⁻⁶⁾ and $p\text{-H}_2$ ⁽⁷⁾ over a wide range of pressures and temperatures. Up to at least 15 bar the solubility divided by the pressure is roughly a constant which decreases linearly with temperature. From these data, liquid hydrogen freezing at one bar is expected to have only 0.03% He gas dissolved in it. We anticipate that D_2 would behave similarly. Additional fractionation in the solid phase could easily lower the He impurity to a few parts per million, and in any case, annealing of the samples at ~ 12 K would further reduce the helium content. Finally, we note that the hcp-fcc transitions which we observed in para-deuterium took place at the same temperatures as were measured⁽⁸⁾ in the absence of a liquid helium environment.

Figure 2 shows diffraction patterns for several samples of as-frozen deuterium at 4 K. The phase diagram predicts that all of these samples should be hexagonal. Surprisingly, the five strongest peaks correspond in position and intensity to those expected for spherical

molecules centered on an fcc lattice. The indices for these cubic peaks are written horizontally. Four of these peaks would also be expected for the hcp structure, but with much different intensities. In addition, there are four weak peaks which are unique to the hcp structure. Indices for the hexagonal peaks are written vertically. The fraction that is hexagonal varies among specimens but it is apparently not related to the para content. On the average, the as-frozen material is about 10% hexagonal and 90% cubic. The unexpected cubic structure has also been observed by other workers,^(9,10) particularly when the solid was formed by freezing the vapor on a cold surface.

Our samples were subsequently annealed by allowing the temperature to rise to about 12 K. This warming caused all of the samples to transform to pure hcp and they remained hcp when cooled back down to 4 K.

Scans of several samples treated in this way are shown in Fig. 3. Twelve hcp peaks were seen, and the intensities were in good agreement with those expected for spherical molecules centered on a hcp lattice. There was no significant variation in peak intensity with para content. No change in the diffraction patterns was observed when the 2 and 29% para-deuterium samples were further cooled to 1.5 K.

For samples of 90 and 96% para-deuterium, a phase change was observed at temperatures in agreement with those in the earlier phase diagram. Scans of several such samples are shown in Fig. 4. The five strong peaks expected for an fcc center-of-mass lattice are seen, together with four weak hcp peaks. In every case there was residual hexagonal material which persisted even though the temperature was cycled repeatedly between 1.5 and 4 K and finally held overnight at 1.5 K.

The five open arrows show the positions of additional peaks expected if the cubic material is ordered into the Pa3 structure. With the statistical accuracy obtained in a single scan, it is not possible to make a definite conclusion as to whether these peaks are present or not. It is clear, however, that these peaks, if present, have intensities much lower than those reported by Mucker et al⁽²⁾.

To improve the statistical accuracy data from five scans were combined and smoothed by averaging adjacent points. The results, much magnified, are shown in the upper curve of Fig. 5. The lower curve shows, for comparison, the results of similar treatment of several scans of the as-frozen material, which is not ordered. Indices of the Pa3 peaks are enclosed in boxes. Statistically significant intensities for four of the five Pa3 peaks were obtained by a least-squares fitting program, and three of them were also revealed when the data were subjected to a cross-correlation analysis using the method devised by Black.⁽¹¹⁾ The latter treatment searches for correlations between the data and the diffractometer resolution function, and is free of any bias as to whether a peak is expected at a given position. The (210) peak was not detected by either technique, and the (221) peak was not found in the cross-correlation analysis, possibly due to its closeness to the hcp (10.3) peak. The remaining three Pa3 peaks were seen by both techniques. Similar cross-correlation analysis of combined data for the as-frozen-cubic and the annealed-hexagonal materials revealed no lines other than those expected for the disordered close-packed structures.

Figure 6 shows a comparison between the observed structure factors and those calculated from the quantum mechanical probability distribution

for $J = 1$, $m_j = 0$ molecules in the $Pa\bar{3}$ space group. The weighted disagreement factor for the squares of the structure factors was 3.2%, which is considered to be very good agreement. The temperature factor obtained in the refinement corresponds to a Debye Θ of 110 K.

During the course of the experiment it was noted that the peaks for the as-frozen cubic material did not occur at quite the expected positions and that furthermore many of the observed peaks were broader than could be explained by the instrumental resolution. All of these effects can be explained by the assumption that there are stacking faults present in the various structures. Both the cubic and hexagonal close-packed structures can be built up by stacking close-packed planes of spheres. There are three possible relative positions for such planes which we can label A, B and C. The sequence ABCABC gives a cubic close-packed structure whereas the sequence ABABAB gives a hexagonal close-packed structure. If the energy difference between these two structures is not very big then there can be mistakes or faults in the stacking sequence of a crystal. Figure 7 shows the two most common stacking faults for the face-centered cubic structure. At left is the sequence for a perfect crystal. In the center is a fault normally called a deformation fault. This could have been produced, for example, by slip along the dotted line. At the right is a fault, known as a growth fault, where at the dotted line the sequence changes from a given face-centered cubic stacking to its twin. Such faults produce peak shifts and peak broadening according to the equations shown on the lower part of the slide. Note particularly that the broadening of the

(111) peak is only slightly more than 40% of the broadening of the (200) peak. Such a difference in the broadening of these peaks would be very difficult to produce by any of the other sources of peak broadening such as particle size or strain. Figure 8 shows similar results for the hexagonal-close-packed structure. Note here that there are no peak shifts and only certain peaks are broadened.

The discrepancies in the line positions for the as-frozen disordered cubic solid were completely resolved when the presence of deformation faults was assumed. Figure 9 shows residual peak breadths after the instrumental resolution has been removed. Note that for the two cubic structures the (111) peak broadening is of the order of 40% of that for the (200) and that for the hexagonal-close-packed structure certain peaks show very little broadening while others show significant broadening. The latter are just the ones expected from the stacking fault analysis. Figure 10 shows the results expressed in terms of the average number of planes between faults. The as-frozen cubic showed both deformation and growth faults with more of the faults being the growth type. The average distance between all faults was 14 planes. The Pa3 structure showed a negligible amount of deformation faulting but growth faults occurred every 27 planes on the average. The hexagonal-close-packed structure showed predominantly deformation faults with the order of 100 planes between faults. Stacking faults are well known in metallurgy and occur frequently in cold-worked metals. It is interesting to see that the same analysis applies to solid hydrogen.

In the course of the experiment, accurate lattice constants were determined for many samples. In the hcp structure the c/a ratio was 1.6317 (very close to the ideal value of 1.6330) and showed no variation with para-concentration. Molar volumes calculated from the lattice constants are shown in Fig. 11. For a given para-concentration, the molar volume was independent of the temperature between 1.5 and 4 K and was the same for the as-frozen cubic and for the annealed hexagonal-close-packed within the accuracy of the experiment. These data were therefore averaged. The molar volume may be seen to decrease linearly as the para-concentration increases. The molar volume for the ordered Pa3 samples was significantly lower than that of either the corresponding hexagonal or as-frozen cubic, indicating a closer packing in this structure.

We may conclude by noting that (as Barrett et al⁽¹²⁾ pointed out) the transition from hexagonal to ordered cubic has all the characteristics of a martensitic transition and that, in particular, it does not go to completion. Also mixtures of fcc and hcp material may be obtained where only hcp is expected, and finally, all structures are susceptible to stacking faults. It may be important to keep those facts in mind in the analysis of experimental data.

1. R. L. Mills, J. L. Yarnell, and A. F. Schuh, *Low Temperature Physics - LT 13*, Boulder 1972, (Plenum, New York, 1973), Vol. 2, p. 203.
2. K. F. Mucker, P. M. Harris, D. White, and R. A. Erickson, *J. Chem. Phys.* 49, 1922 (1968).
3. Werner Press, *Acta Cryst.* A29, 257 (1973).
4. W. B. Streett, R. E. Sonntag, and G. J. Van Wylen, *J. Chem. Phys.* 40, 1390 (1964).
5. N. E. Greene and R. E. Sonntag, *Advances in Cryogenic Engineering* (Plenum, New York, 1968), Vol. 13, p. 357, Proc. of the 1967 Cryogenic Eng. Conf., Stanford University, Aug. 21-23, 1967.
6. C. M. Sneed, R. E. Sonntag, and G. J. Van Wylen, *J. Chem. Phys.* 49, 2410 (1968).
7. R. E. Sonntag, G. J. Van Wylen, and R. W. Crain, Jr., *J. Chem. Phys.* 41, 2399 (1964).
8. A. F. Schuch and R. L. Mills, *Phys. Rev. Lett.* 16, 616 (1966).
9. A. E. Curzon and A. J. Mascall, *Brit. J. Appl. Phys.* 16, 1301 (1965).
10. O. Bostanjoglo and R. Kleinschmidt, *J. Chem. Phys.* 46, 2004 (1967).
11. W. W. Black, *Nucl. Instr. Meth.* 71, 317 (1969).
12. C. S. Barrett, L. Meyer, and J. Wasserman, *J. Chem. Phys.* 45, 834 (1966).

Deuterium

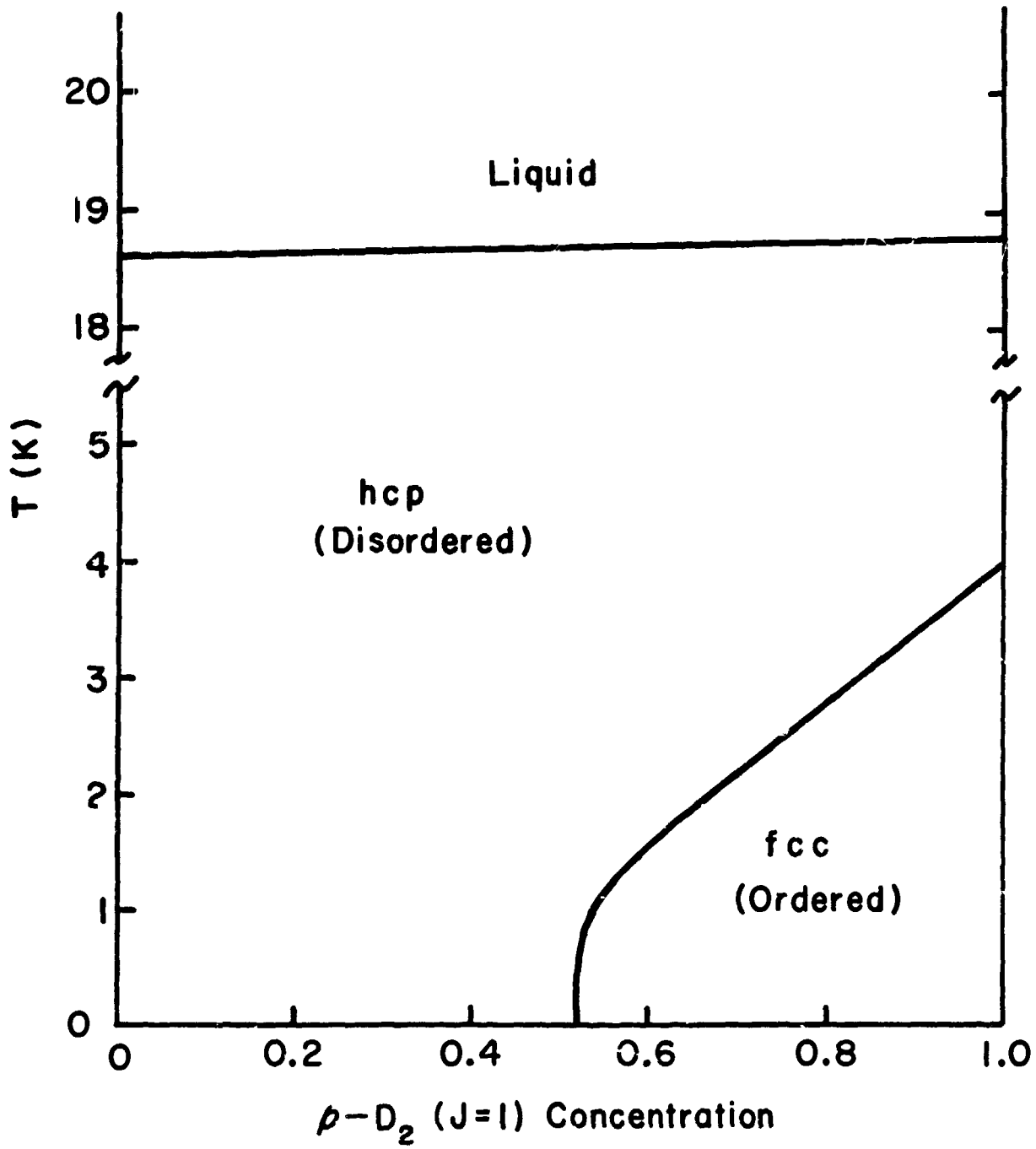


Fig. 1.

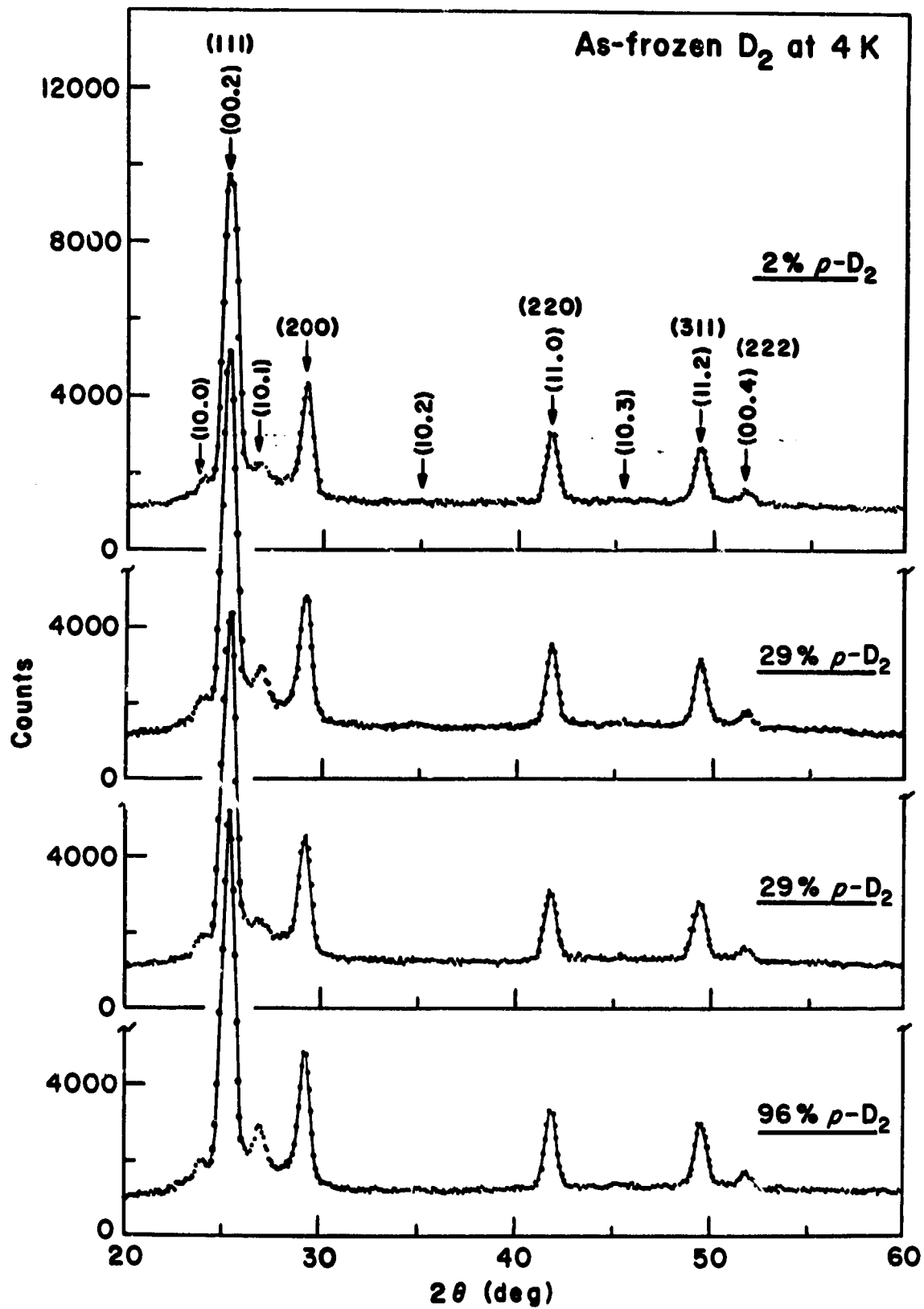


Fig. 2.

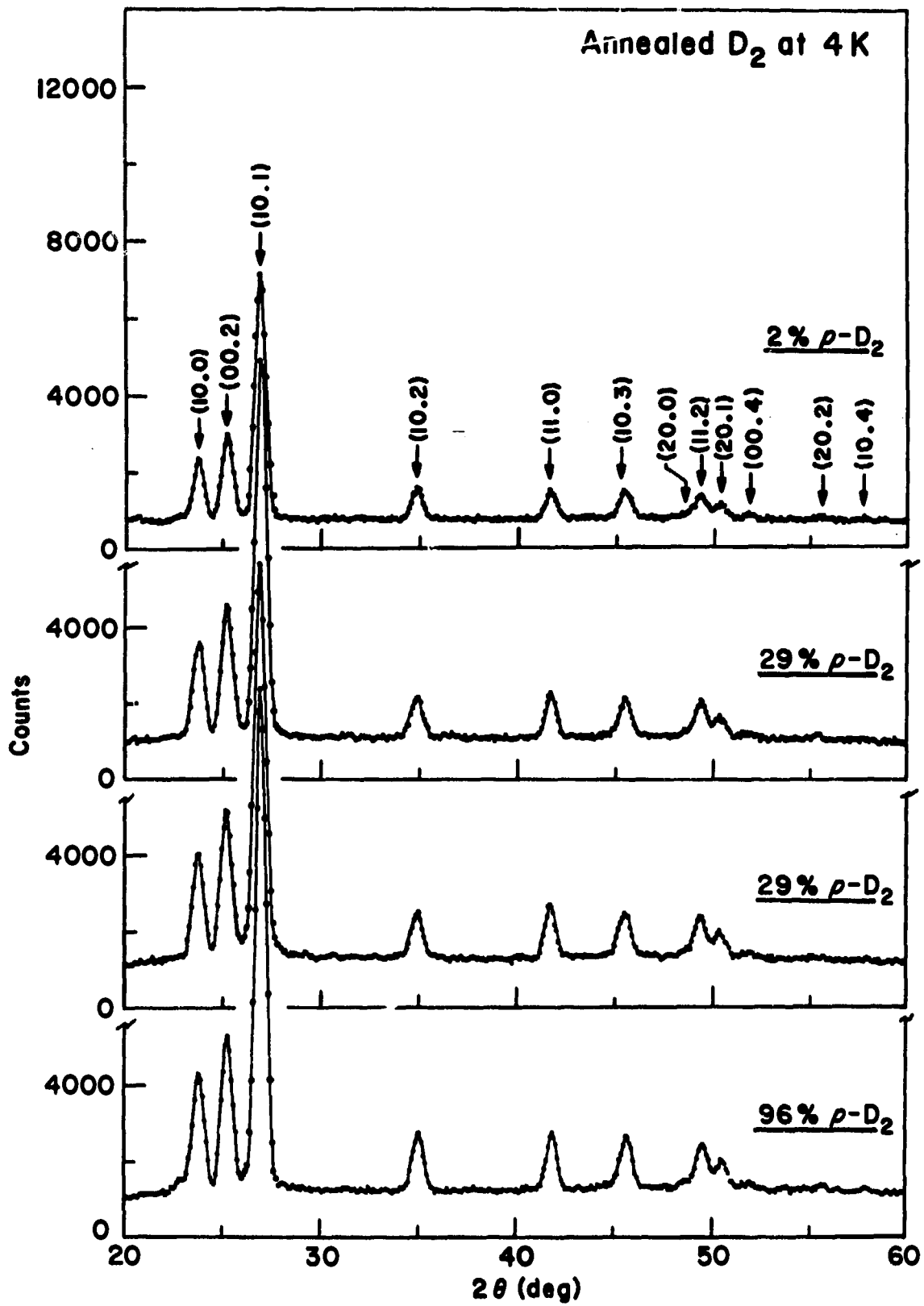


Fig. 3.

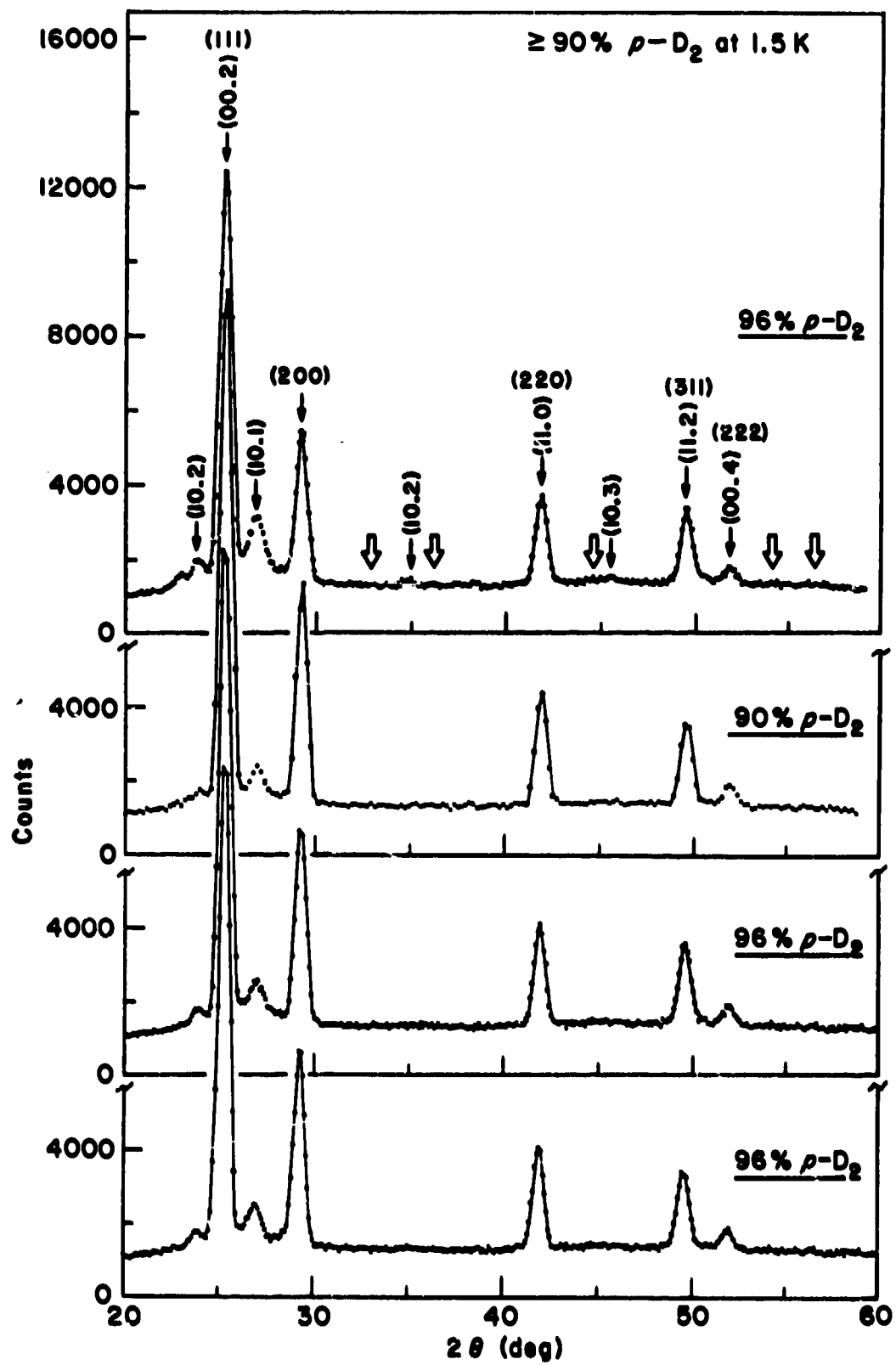


Fig. 4.

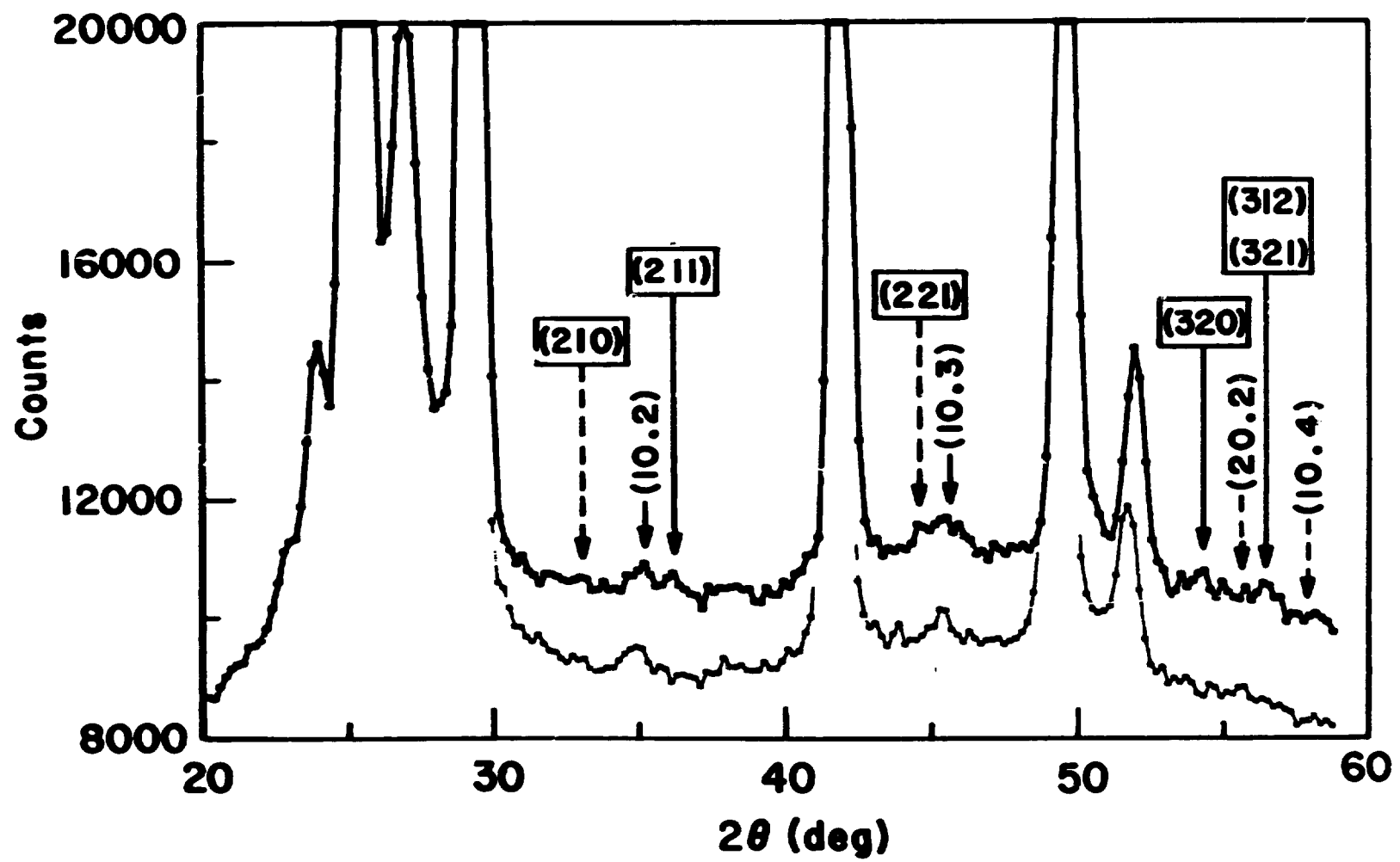


Fig. 5.

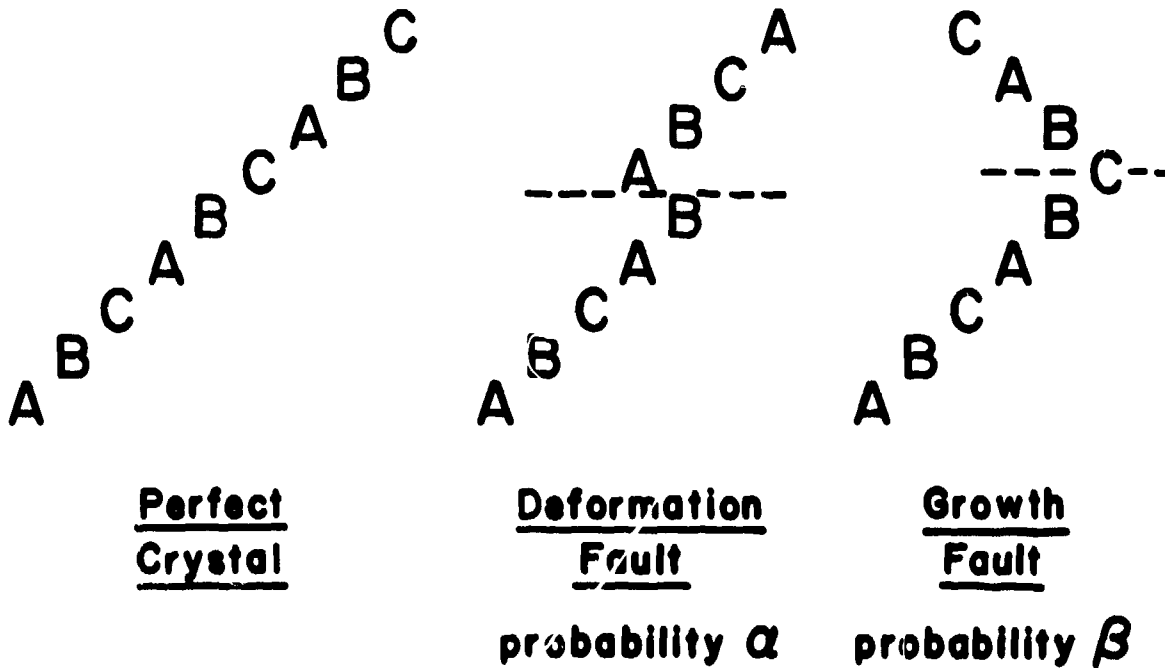
**Observed and Calculated Structure
Factors for Ordered Cubic D_2**

hkl	$\geq 90\% \text{ p-}D_2$	
	F_o	F_c^a
111	6.026	5.931
200	5.240	5.358
210	-----	0.306
211	0.266	0.287
220	3.536	3.558
221	0.222	0.226
311	2.646	2.599
222	2.421	2.337
302	0.419	0.488
321, 312	0.415	0.475
$a(\text{\AA})$	3.0760	
$D(\text{\AA}^2)$	6.514	
R_{VF}^2	0.032	

^a Quantum mechanical form factor for $J = 1, m_j = 0$ molecules in $Fm\bar{3}$ space group.

Fig. 6.

fcc Stacking Faults



Peak Shift $\Delta = \alpha \frac{90 \lambda \sqrt{3}}{\pi^2} \tan \theta C_{hkl}$

Peak Breadth $b = (1.5\alpha + \beta) \frac{90 \lambda}{\pi a \cos \theta} V_{hkl}$

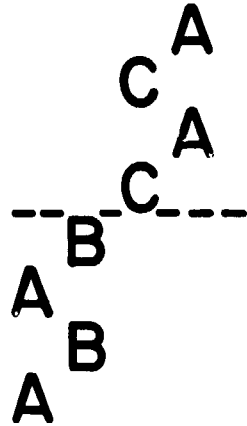
h k l	C_{hkl}	V_{hkl}
1 1 1	-0.035	0.43
2 0 0	+0.069	1.00
2 2 0	-0.035	0.71
3 1 1	+0.013	0.45
2 2 2	+0.017	0.43

Fig. 7.

hcp Stacking Faults

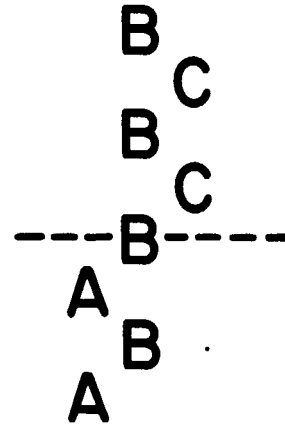


Perfect
Crystal



Deformation
Fault

probability α



Growth
Fault

probability β

Peak Shift – None

Peak Breadth

$$b = 0, H - K = 3N$$

$$b = (3\alpha + \beta) \frac{90 \lambda^2 |L|}{\pi c^2 \sin 2\theta}, \begin{cases} H - K \neq 3N \\ L \text{ odd} \end{cases}$$

$$b = (3\alpha + 3\beta) \frac{90 \lambda^2 |L|}{\pi c^2 \sin 2\theta}, \begin{cases} H - K \neq 3N \\ L \text{ even} \end{cases}$$

Fig. 8.

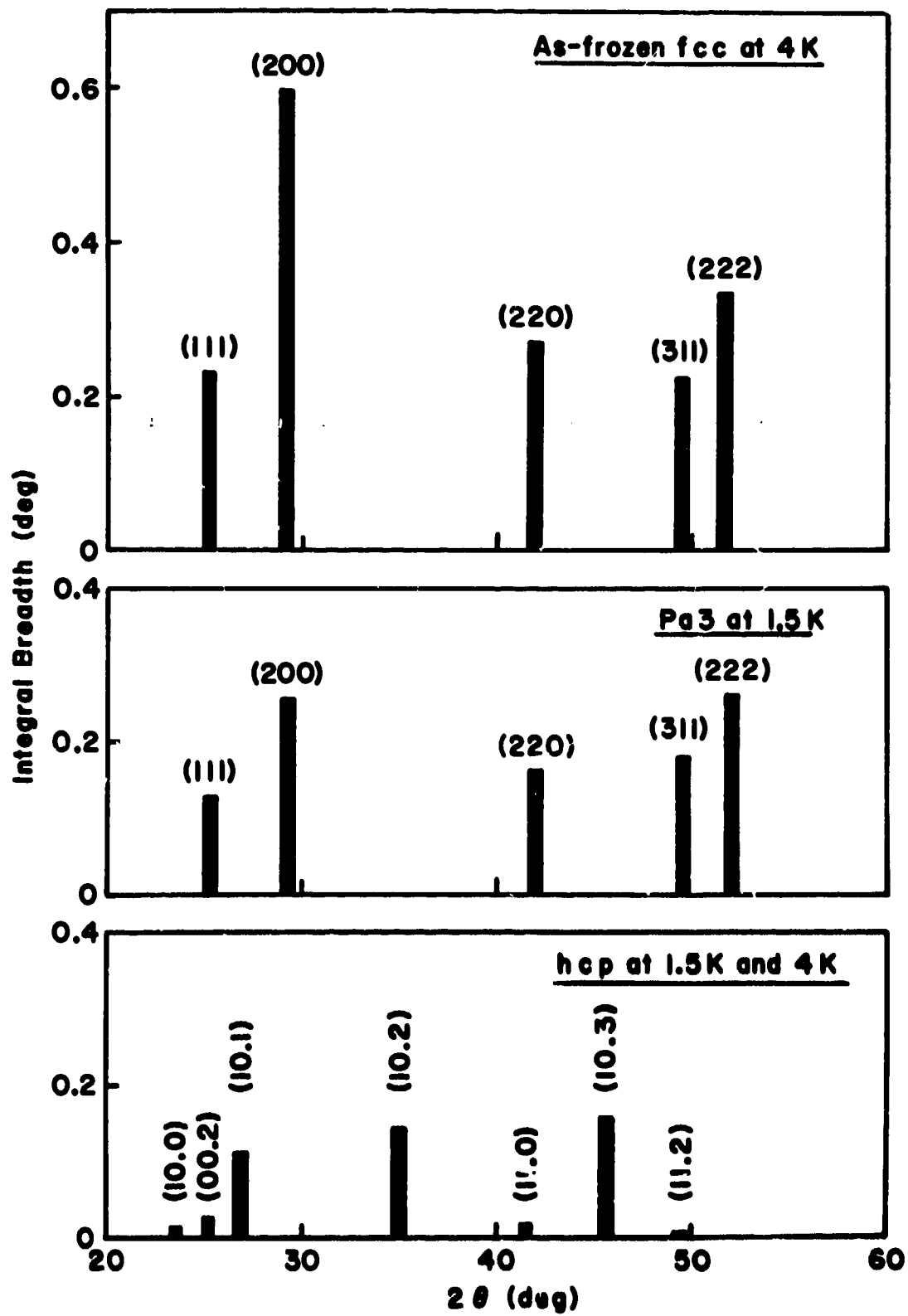


Fig. 9.

**AVERAGE NUMBER OF PLANES
BETWEEN FAULTS**

	DEFORMATION FAULTS	GROWTH FAULTS	ALL FAULTS
AS-FROZEN CUBIC AT 4 K	75	18	14
PA 3 AT 1.5 K	> 600	27	27
H C P AT 1.5 AND 4 K	95	>> 95	95

Fig. 10.

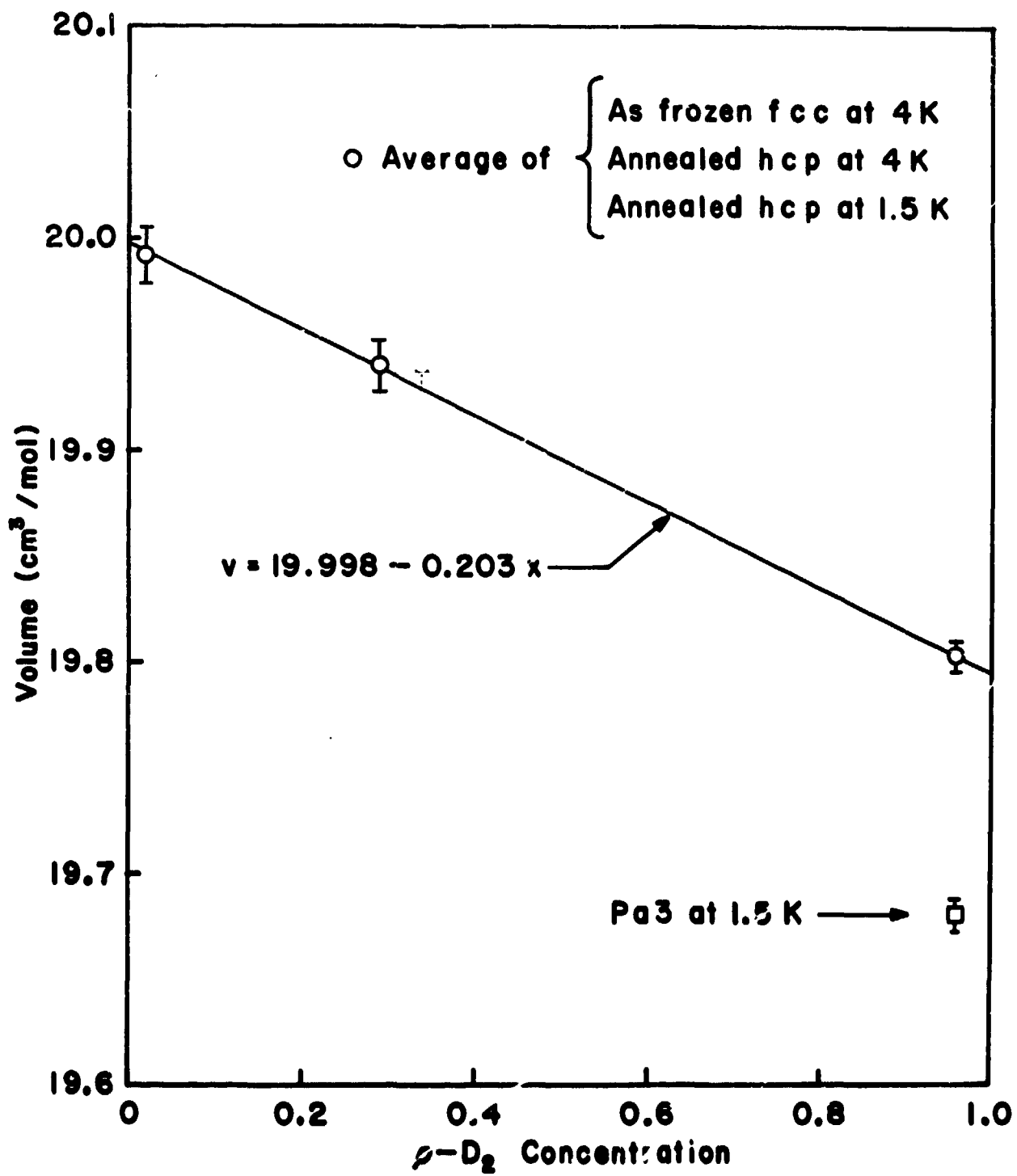


Fig. 11.